Available online at www.sciencedirect.com

ScienceDirect

Energy Procedia 92 (2016) 96 – 102

Energy Procedia

6th International Conference on Silicon Photovoltaics, SiliconPV 2016

# Efficiency improvement by charged-insulator layers for IBC-SHJ cells

Takefumi Kamioka[a,]*, Yutaka Hayashi[a], Kyotaro Nakamura[b], Yoshio Ohshita[a]

[a]*Toyota Technological Institute, 2-12-1 Hisakata, Tempaku, Nagoya, 468-851, Japan*
[b]*Meiji University,1-1-1 Higashimita, Tama, Kawasaki, 214-8571, Japan*

**Abstract**

A novel approach has been proposed to solve conversion efficiency degradation due to recombination loss at a gap region between p/i- and n/i-aSi:H layers in an interdigitated back contact Si heterojunction (IBC-SHJ) cell architecture. In our approach, a charged-insulator layer is newly introduced to cover the i-aSi:H on the gap region. Our simulation demonstrates that this leads to suppression of the recombination at the gap region, resulting in a significant improvement in the efficiency. Fixed-charge ($Q_f$) with density of around $10^{12}$ cm$^{-2}$ almost fully recovers the efficiency even with a low-quality surface at the gap around with the interfacial defect density of $10^{12}$ cm$^{-2}$eV$^{-1}$. The decrease in the recombination is owing to the field-effect passivation induced by the $Q_f$. The recovery in the efficiency by $Q_f$ still works even though the quantum effects is considered, which causes some modification in the carrier distribution at the hetero-interface. Such charged-insulators are feasible by already existing materials such as Si nitride. In addition, this charged insulator architecture allows easy alignment for the backside structure. Thus, this proposal will be easily adopted for a mass production where the relaxed design rule is mandatory.


Peer review by the scientific conference committee of SiliconPV 2016 under responsibility of PSE AG.

*Keywords:* solar cell; silicon; amorphous silicon; heterojunction; back contact; fixed charge; charged insulator

## 1. Introduction

Interdigitated back contact Si heterojunction (IBC-SHJ) cells have been of particular interest because of their high potential as high-efficiency cells [1,2]. The advantage of this architecture is high short-circuit current ($J_{sc}$) due to

* Corresponding author. Tel.: +80-52-809-1877; fax: +80-52-809-1878.
*E-mail address:* t-kamioka@toyota-ti.ac.jp


Peer review by the scientific conference committee of SiliconPV 2016 under responsibility of PSE AG.
doi:10.1016/j.egypro.2016.07.035

avoidance of shading effects by front electrode grids. However, high-quality surface passivation on a gap surface between an emitter and a collector has been inevitable for high open-circuit voltage ($V_{oc}$).

From the viewpoint of a mass production, there are many obstacles mainly coming from the process cost. Since high-cost processes such as a photolithography pattering are not to be used, the gap distance between an emitter and a collector cannot be narrowed. This gap region acts as a dead region, which causes sometimes efficiency loss. This problem becomes serious when the passivation quality is low. It has been reported by numerical simulation that this gap problem also occurs even if a "p/n-overlapping" structure is applied [3]. To minimize this gap-induced efficiency loss, keeping a high-quality passivation is required for any variation of IBC-SHJ structures [4].

To utilize a field-effect passivation [5-6] is another way to keep and/or improve the passivation quality. The filed-effect passivation is induced by fixed-charges in an insulator. However, there has been no report on the effect of fixed-charges in a passivation layer at the rear-side of an IBC-SHJ cell.

In this work, we propose a novel architecture to solve this gap problem, which has a charged-insulator/i-aSi:H stack capping over the gap region of an IBC-SHJ cell [Fig. 1(b)]. We numerically demonstrate the effect of the charged-insulator layer on the cell performance. From the result, it is suggested that this architecture can be easily applied to an existing fabrication process.

## 2. Simulation method

Simulated device models are shown in Fig. 1. The base structure of our novel one is an n-type IBC-SHJ cell, but an insulator in which fixed-charge is embedded between an emitter and a collector region. Here, an example of this "charged-insulator (C-INS)" is Si nitride ($SiN_x$). For numerical modeling, $Q_f$ is assumed to be located at the i-aSi:H/charged-insulator interface. The location in the thickness of $Q_f$ in the charged-insulator does not result in the different passivation effect. A 1-nm-thick defective layer [7] is inserted between i-aSi:H and cSi to model the interface defect density ($D_{it}$). Here $D_{it}$ at the front-side i-aSi:H/cSi interface is fixed at $10^{10}$ cm$^{-2}$eV$^{-1}$. The electronic properties of other materials were followed our previous models [4,8]. A 2D device simulator "ATLAS" [9] was used for numerical analysis of the cell performance. The roles of the charged-insulator were studied by changing $Q_f$ for different gap distances ($W_g$) and $D_{it}$'s.

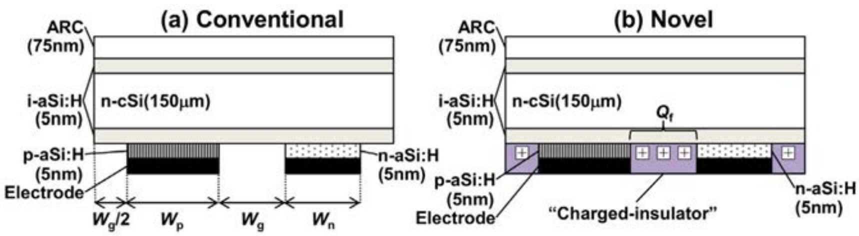


Fig. 1. Schematics of IBC-SHJ cell models; (a) a conventional structure and (b) our newly proposed structure in which charged-insulator layers are capping over gap regions. No surface texture is considered. The widths of emitter ($W_p$) and collector ($W_n$) are 1200 and 500 μm, respectively.

## 3. Results and discussion

### *3.1. Effect of the fixed-charge density on cell performance*

Simulated efficiency ($\eta$) as a function of gap distance ($W_g$) is shown in Fig. 2 for the conventional and the novel structures. Here, the fixed charge density ($Q_f$) is set at $10^{11}$ and $10^{12}$ cm$^{-2}$. For the conventional structure, the efficiency decreases significantly by widening gap. At $W_g$ = 100 μm, which is the same order in a mass production line, over 20% degradation is expected for a poor interface quality ($D_{it}$ = $10^{12}$ cm$^{-2}$eV$^{-1}$). For the novel structure, however, almost no degradation is expected (only a few %). This result clearly demonstrates that our novel structure is an effective approach to improve the efficiency.

Relation between the cell parameters and $Q_f$ is shown in Fig. 3 for different $D_{it}$'s and $W_g$'s. High $Q_f$ leads to high efficiency. This is attributed to the increase in $V_{oc}$, $J_{sc}$ and fill factor (*FF*). The mechanism for the increase in the efficiency will be discussed in detail below. Especially, $Q_f > 10^{12}$ $cm^{-2}$ is critical condition for the efficiency enhancement. Each cell parameter is improved to that at an almost gapless condition ($W_g$ = 1 μm).

It is noteworthy that introduction of high $Q_f$ is effective even for the low quality interface ($D_{it} = 10^{12}$ $cm^{-2}eV^{-1}$) and for large $W_g$ (equals to the substrate thickness of 150 μm). Thus, IBC-SHJ with the charged-insulator architecture proposed here could be a booting technology to start a mass production phase. In addition, the charged insulator can overlap an emitter electrode and a collector electrode, resulting easy alignment and a less gap between the electrodes. This is an advantage compared to the "p/n-overlapping" structure. In the "p/n-overlapping" structure an extra marginal gap for alignment between the emitter electrode and n-aSi:H layer is required, and this results in a larger gap between the electrodes than the charged insulator architecture.

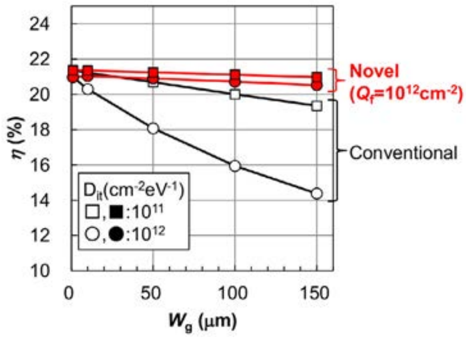


Fig. 2. Comparison between a conventional and the novel structures in the simulated efficiency as a function of gap distance ($W_g$). Interface defect density ($D_{it}$) at the rear i-aSi:H/c-nSi is a parameter.

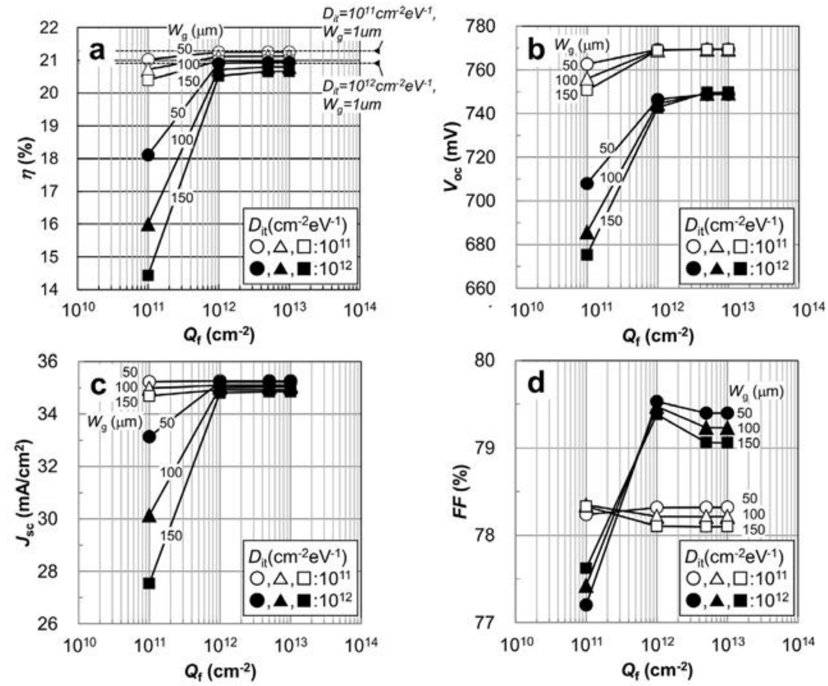


Fig. 3. Calculated cell parameters as a function of fixed-charge density ($Q_f$) for different gap distances ($W_g$) and interface defect densities ($D_{it}$) at the rear i-aSi:H/c-nSi interfaces. The thickness of i-aSi:H is 5 nm and impurity (donor) concentration of the substrate is $1.9\times10^{15}$ $cm^{-3}$.

*3.2. Detailed analysis on the effect of the fixed-charge*

In order to understand the mechanisms of the above fixed-charge-induced effect, the band diagram is analyzed across the n-cSi/i-aSi:H/charged-insulator stack [Fig. 4(a)]. Silicon nitride is one of the candidates for the positively charged insulator [10]. As $Q_f$ increases from $10^{11}$ to $10^{12}$ $cm^{-2}$, the band bending at the cSi side of the interface becomes strong to downwards. The polarity of the electric field acts to repel the minority carriers (holes) from the interface, leading to the decrease in hole concentration near the interface significantly while the increase in majority carrier concentration [Fig. 4(b)]. As a result, the recombination at the interface significantly decreases around 2 orders of magnitude [Fig. 4(c) and (d)]. This leads to the significant increase in all cell parameters. The steep change around $Q_f = 10^{12}$ $cm^{-2}$ means that fixed-charge density reaches high enough for accumulating majority carriers. The sensitivity of this trend will depend on the base doping of Si substrate.

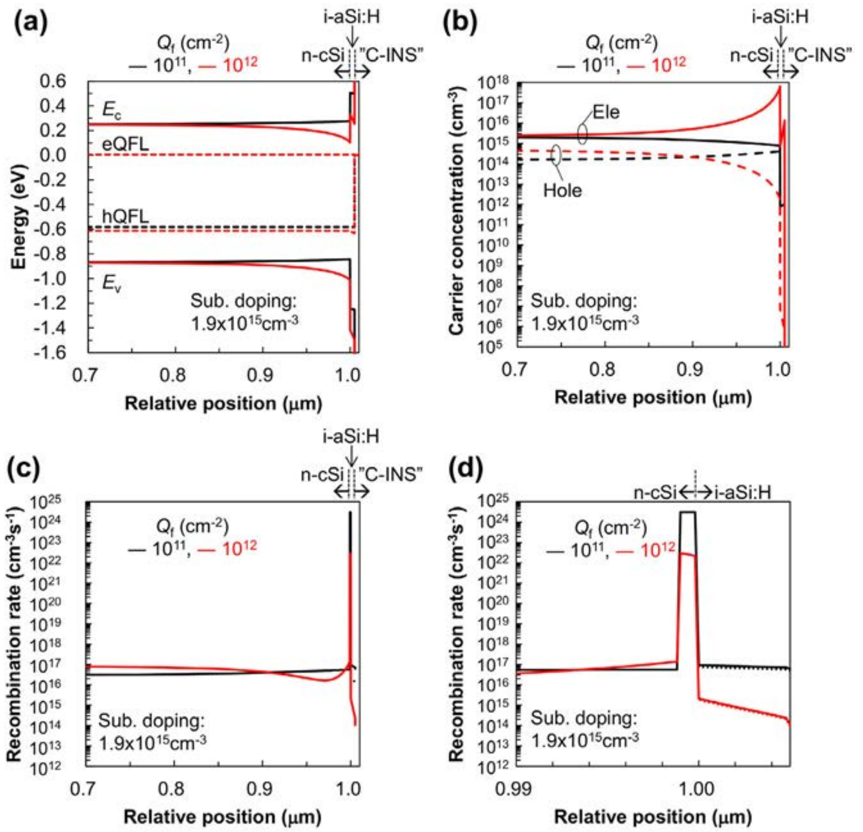


Fig. 4. Profiles for (a) band diagrams, (b) carrier concentrations, and (c) total recombination rate for low and high $Q_f$ across the n-cSi/i-aSi:H/charged-insulator ("C-INS") stack. (d) is the zoom-up view of (c) near the n-cSi/i-aSi:H interface. All data are obtained under short-circuit condition.

Another option to control the band-bending is to change the doping concentration in the i-aSi:H layer covering the gap region. Fig. 5 shows the $Q_f$ dependence on the cell parameters for different donor concentration ($N_d$) in the rear i-aSi:H layers. In this simulation, all donors are assumed to be completely ionized. As the doping concentration increases in the i-aSi:H layer, all cell parameters are improved. This is due to the field-effect passivation becomes dominant. The critical values of $Q_f$ for the efficiency recovery decreases for large $N_d$. This means that the required $Q_f$ in the charged insulator can be reduced. In practice, however, the ionization of the dopant atoms in the aSi is incomplete [11]. In addition, the increase of the doping concentration also leads to the increase of the defect concentration in the layer, resulting in the degradation of the passivation quality [12]. Thus, this approach will not be effective in the actual case.

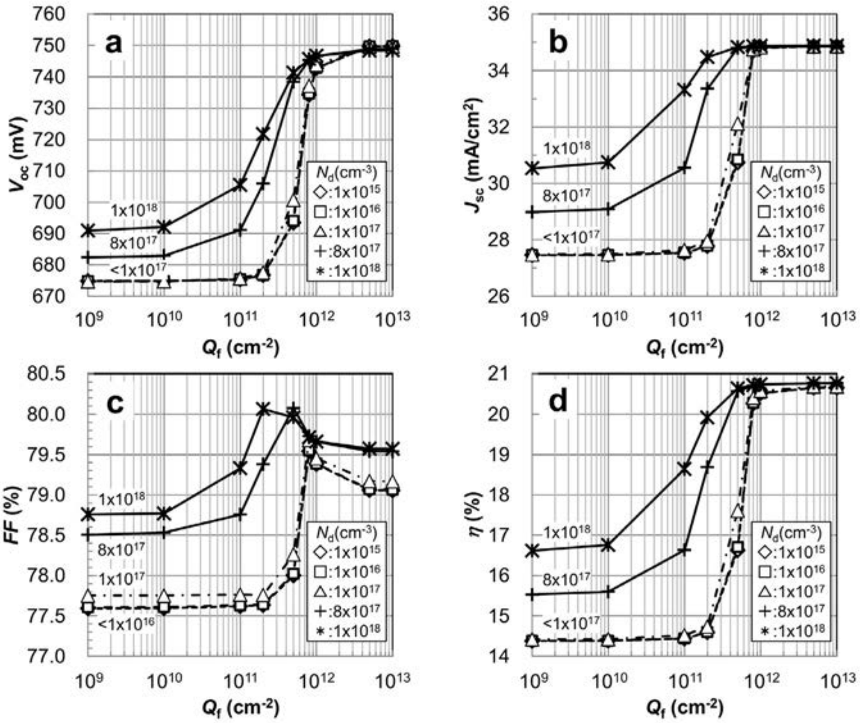


Fig. 5. Cell parameters as a function of $Q_f$ for different donor concentrations ($N_d$) in the rear i-aSi:H layer on the gap region.

The control of the band bending is a critical factor for this recovery effect. Such band bending is expected to be modified if quantum effects at the hetero-interface are considered since the carrier distribution is modified compared with that for the classical model. The importance of considering the quantum effects for detailed understanding the device physics was reported in our previous work [8]. Here we investigate whether or not the recovery effect by $Q_f$ is still effective even though the quantum transport model is adopted. The density gradient model [13] was used for this purpose. This model is based on the classical drift-diffusion equation but added with a quantum potential term ($\Lambda$), described as,

$$\Lambda = -\frac{\gamma h^2}{12m}\left[\nabla^2 \log n + \frac{1}{2}\left(\nabla \log n\right)^2\right], \qquad (1),$$

where $h$ denotes the Plank's constant, $m$ the effective mass of carrier, $n$ the carrier concentration. The fitting parameter, $\gamma$, depends on the system configuration such as material combinations and geometries. The classical model corresponds to $\gamma = 0$ and larger $\gamma$ means the quantum effects becomes prominent. Fig. 6 shows the comparison between the classical and quantum models of the $Q_f$ dependence on the cell parameters. The result shows that at any $\gamma$ value, the critical $Q_f$ value to an efficiency recovery is the same as $10^{12}$ cm$^{-2}$ for the classical and the quantum model, although the exact values are slightly different. This means that the effect of $Q_f$ on the band bending is much stronger than that of the modified carrier distribution due to the quantum effects.

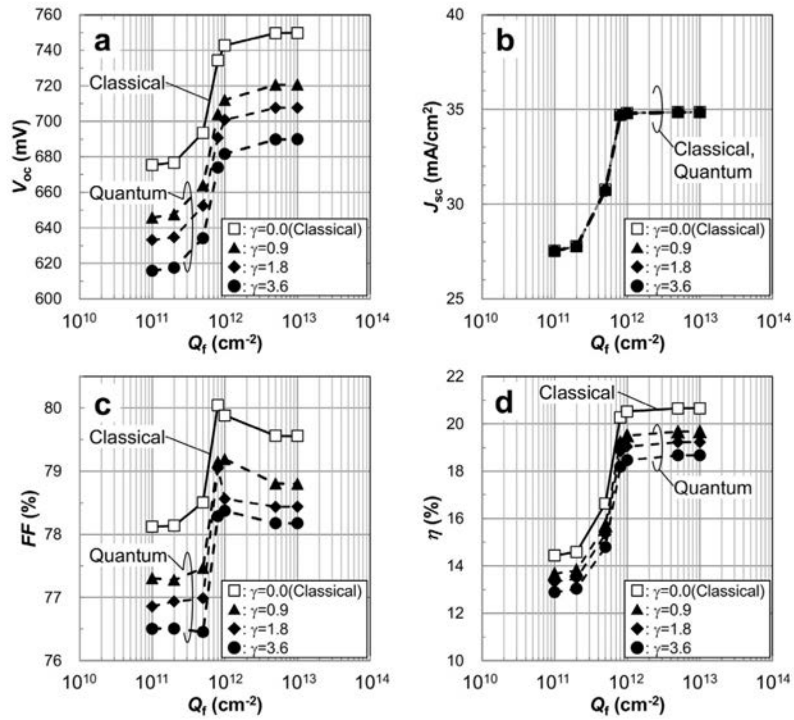


Fig. 6. Comparison of the effects of $Q_f$ on the cell performance between the classical and the quantum transport models. Here different values of fitting parameter in the quantum potential term, $\gamma$, are investigated. The classical model corresponds to $\gamma = 0$.

## 4. Conclusion

A novel structure for supporting robustness in keeping high efficiency was numerically demonstrated for an IBC-SHJ architecture. A charged-insulator capping over the gap region is quite effective for efficiency improvement. A critical value of $Q_f$ in the charged insulator is around $10^{12}$ $cm^{-2}$ for the impurity concentration of substrate of $1.9\times10^{15}$ $cm^3$. This is mainly due to the reduction of recombination at the gap region by band engineering. This approach could be adoptable for any passivated contacted cells with all back contact structures.

## Acknowledgements

This work was partly supported by the New Energy and Industrial Technology Development Organization (NEDO) under the Ministry of Economy, Trade and Industry of Japan.

## References

[1] K. Masuko, M. Shigematsu, T. Hashiguchi, D. Fujishima, M. Kai, N. Yoshimura, T. Yamaguchi, Y. Ichihashi, T. Mishima, N. Matsubara, T. Yamanishi, T. Takahama, M. Taguchi, E. Maruyama and S. Okamoto, "Achievement of more than 25% conversion efficiency with crystalline silicon heterojunction solar cell", IEEE J. Photovoltaics, 4 (6), 1433-1435 (2014).

[2] J. Nakamura, N. Asano, T. Hieda, C. Okamoto, H. Katayama, and K. Nakamura, "Development of heterojunction back contact Si solar cells", IEEE J. Photovoltaics, 4 (6), 1491-1495 (2014).

[3] H. Noge, K. Saito, A. Sato, T. Kaneko, and M. Kondo, "Two-dimensional simulation of interdigitated back contact silicon heterojunction solar cells having overlapped p/i and n/i a-Si:H layers", Jpn. J. Appl. Phys., 54 (8S1), 08KD17-1-08KD17-6 (2015).

[4] T. Kamioka, Y. Hayashi, K. Nakamura, and Y. Oshita, "Simulation of interdigitated back-contact silicon heterojunction solar cells with quantum transport model", Jpn. J. Appl. Phys., 54 (8S1), 08KD07-1-08KD07-6 (2015).

[5] S. W. Glunz, D. Biro, S. Rein, and W. Warta, "Field-effect passivation of the $SiO_2$-Si interface", J. Appl. Phys. 86 (1), 683-691 (1999).

[6] B. Hoex, S. B. S. Heil, E. Langereis, M. C. M. van de Sanden, and W. M. M. Kessels, "Ultralow surface recombination of c-Si substrates passivated by plasma-assisted atomic layer deposited $Al_2O_3$", Appl. Phys. Lett. 89 (4), 042112-1-042112-3 (2006).

[7]A. S. Gudovskikh, S. Ibrahim, J. –P. Kleider, J. Damon-Lacoste, P. Roca i Cabarrocas, Y. Veschetti, and P. –J. Ribeyron, "Determination of band offsets in a-Si:H/c-Si heterojunctions from capacitance-voltage measurements: Capabilities and limits", Thin Solid Films 515 (19), 7481-7485 (2007).

[8] Y. Hayashi, D. Li, A. Ogura, and Y. Oshita, "Role of i-aSi:H layers in aSi:H/cSi heterojunction solar cells", IEEE J. Photovoltaics 3 (4), 1149-1155 (2013).

[9] Atlas ver. 5.18.3.R, Silvaco Inc., Santa Clara, CA, USA, 2012.

[10] V. Sharma, C. Tracy, D. Schroder, S. Herasimenka, W. Dauksher, and S. Bowden "Manipulation of K center charge states in silicon nitride films to achieve excellent surface passivation for silicon solar cells", Appl. Phys. Lett. 104 (5), 053503-1-053503-4 (2014).

[11] M. Stutzmann, D. K. Biegelsen, and R. A. Street, "Detailed investigation of doping in hydrogenated amorphous silicon and germanium", Phys. Rev. B 35 (11), 5666-5701 (1987).

[12] M. Tanaka, M. Taguchi, T. Matsuyama, T. Sawada, S. Tsuda, S. Nakano, H. Hanafusa, and Y. Kuwano, "Development of new a-Si/c-Si heterojunction solar cells: ACJ-HIT (artificially constructed junction-heterojunction with intrinsic thin-layer)", Jpn. J. Appl. Phys. 31 (11), 3518-3522 (1992).

[13] A. Wettstein, A. Schenk, and W. Fichtneret, "Quantum device-simulation with the density-gradient model on unstructured grids", IEEE Trans. Ele. Dev. 48 (2), 279-284 (2001).